3D object comparison based on shape descriptors

S. Biasotti and S. Marini

3D object comparison based on shape descriptors

Abstract

Due to the recent improvements to 3D object acquisition, visualisation and modelling technologies, the number of 3D models available on the web is more and more growing, and there is an increasing demand for tools supporting the automatic search for 3D objects in digital archives. Traditional methods for 3D shape retrieval roughly filter shape information or perform a punctual comparison of models.

In this paper, we discuss on the advantages of approaching the shape matching problem through 3D graph-like descriptors, which decompose the shape into relevant subparts. In our approach, shapes are compared using a graph matching technique that includes a structured process, which identifies the most similar object portions. In particular, we investigate on the properties of these descriptors and of our matching method in the CAD context.

Key words: Shape similarity – 3D object retrieval - graph matching

1   Introduction

The needs to extract knowledge from massive volumes of digital content rapidly increases and new forms of content are coming in evidence, such as 3D animations and virtual or augmented reality. Whilst it has become relatively easier to generate 3D information and to interact with the geometry of shapes, it is harder to structure, filter, organise and retrieve it. These considerations are changing the approach to 3D object modelling. Until now a primary challenge in computer graphics has been how to build

and render complete and effective models, now the key issue is how to find and interpret them. In this sense, methods for automatically extracting the semantic content of digital shapes and generating shape models in which knowledge/semantics is explicitly represented will become more and more necessary. This will allow browsing the web or digital object repositories using enhanced search engines not simply based on text-searches but on shape and semantics (e.g., content and context based search engines capable of answering semantics-based queries) [53].

In our understanding the knowledge of a digital shape may be organised at three different levels of representation: *geometric*, *structural* and *semantic* level [15]. A first organisation of the shape data into a computational structure gives access to the *geometric level* of representation, where different types of geometric models can be used to represent the same object form. As examples, we can list polygons, surface models (splines, NURBS, implicit surfaces,…) [34], solid models (3D mesh, Brep, CSG) [22][28][36], clusters of pixels or voxels (shapes segmented within an image or volume) [36], etc. In a geometric model, topological and geometric information are coded explicitly or implicitly in a computer processable structure.

Then, a *structural level* of representation is reached by organising the geometric information and/or shape data to reflect and/or make explicit the association between parts/components of shapes. Examples of structural models are: multi-resolution and multi-scale models [27], curvature based surface decompositions [52][14], topological decompositions [12][13], shape segmentations, etc..

At the highest level of segmentation, the *semantic* one, there is the association of a specific semantics to structured and/or geometric models through annotation of shapes, or shape parts, according to the concepts formalised by the semantic domain. Therefore, a semantic model is the representation of a shape embedded into a specific context.

The method discussed in this paper approaches the problem of using a structural representation for shape comparison purposes. The first step to fulfil this task is to associate a signature, that is a so-called shape descriptor, to a geometric model. In particular, we would desire that the chosen shape descriptor concisely represents the shape features, is invariant to rigid and similarity transformations, is insensitive to noise and small extra feature, is robust with respect to topological deformations, is suitable for multi-scale analysis and is computationally efficient and simple to store. Moreover, it is our opinion that a signature that organises the object shape in a topologically consistent framework provides a relation between shape structure and semantics. Several methods have been proposed to extract the salient information stored in a model; such as descriptors based on shape distributions [33], spherical harmonics [16][39], statistical distribution of the shape points in the space [48] or the high-curvature regions [20], while others try to organise and interpret the shape features through a graph representation, such as skeletal curves [46] and Reeb graphs [5][21][42]. In particular, we will discuss on the advantage of considering a skeleton based representation of the shape as the signature for approaching the 3D shape comparison problem and on the possible extension of the application domain from free-form models to mechanical ones. Furthermore, we will give a novel interpretation of

our approach, showing that the heuristic method we presented in [6] may be deduced from the more general problem of approximating the maximum common sub-graph [30]; in addition, the heuristic choices we proposed in [6] can be modularly inserted in a general methodology and other approximations may be introduced.

The reminder of this paper is organised as follows. First, an overview of the existing skeletal representations and their use on shape representation and retrieval is proposed, focusing, in particular, on the Reeb graph and the matching approaches based on that structure. Then, our approach to 3D shape comparison is described and arranged in the general graph isomorphism context. Examples and results are proposed in section 4 and compared with those obtained through the spherical harmonics approach in [16]; in addition, the suitability of our method for object matching is discussed. Conclusions and future developments end the paper.

2   Related Work on shape representation and retrieval

Existing techniques can represent the geometry of a shape with high detail, typically through a dense mesh of simple basic elements such as triangles, tetrahedra, etc. Such meshes can approximate the geometry of a shape arbitrarily well, but they fail in describing the morphological structure of the shape, which has a fundamental importance for shape classification and understanding. On the contrary, iconic models, intended as concise, part-based representations of a shape, provide more structured descriptions, even if sometimes less accurate. In this context shape distributions [33], which evaluate the distribution on the surface of a shape function that measures the

geometric properties of the model, and spherical harmonics [16] are expressive tools. The latter descriptor, in particular, decomposing the model into a collection of functions defined on concentric spheres with respect the centre of mass, is invariant to object rotations. The original shape cannot be recovered from these shape descriptors but comparison may be efficiently accomplished using traditional distances between functions. Furthermore, these descriptors do not identify the correspondence between the most similar object sub-parts preventing any reasoning based on the shape structure (e.g.: reasoning about building differences between mechanical artefacts).

In advanced fields, such as virtual human modelling, available modelling tools to represent structured geometry are focused on adding a skeleton to the 3D geometry in order to animate it and provide different degrees of realism (from segmented non-deformable bodies to anatomically accurate deformable meshes). In addition, there has been a considerable amount of work in the literature on extracting critical features (point, integral lines, etc.) from 2D scalar fields describing grey-level images and terrains, and more recently some work has been done on volume data, again on extracting a critical net or on representing the topological structure of the iso-surfaces through the so-called contour tree.

2.1 Skeletal descriptions

A skeletal structure should encode the decomposition of a shape into relevant parts, or features, which may have either a geometric or an application-dependent meaning. Therefore, it is important to detect salient features over non-significant ones and define a mapping between the skeleton and the full geometry, so that the two levels can be

easily interchanged. Moreover, we expect that a skeletal representation is *topologically equivalent* to the original model, *stable*, in the sense that local changes of the shape should be locally reflected on the skeleton and *invariant* to the object position [32]. Skeletons have been studied independently in image analysis by using a discrete geometry approach and in geometric modelling by using *continuous* computational geometry techniques.

In computer graphics literature no general definition of skeleton exists and many different skeletal structures have been defined. The most popular skeletal representation of a bi-dimensional shape is the Medial Axis (MA) or Symmetry Set [32], which was described by Blum [7] as a fire front which starts at the boundary of the shape and propagates isotropically towards the interior. Then, the medial axis is defined by the locations at which the fire fronts collide. The power of this representation is that the shape boundary and its MA are equivalent and the one can be computed from the other (the original shape can be recovered from its medial axis using a simple distance transform); therefore, a two-dimensional object is effectively compressed into a one-dimensional graph-like structure. The notion of shock graph [23] extends that of medial axis, associating to each arc of the MA the direction of increase of the distance transform, see figure 1(a,b). As discussed in [18], both representation methods are independent of the object position and provide a concise description that naturally decomposes the shape in its more meaningful portions. Moreover, the MA is sensitive to tiny perturbations of the boundary; therefore extra edges may appear in the graph with no distinction between main and secondary features [1]. To solve this problem and

highlight the portions of the skeleton that correspond to the shape part with higher perceptual relevance, in [1] a method for pruning the medial axis of 2D and 3D triangulation has been provided. However, when calculated for a 3D shape, these structures are more complex and contain not only lines but also surface elements [37], figure 1(c), and their extraction is computationally expensive.
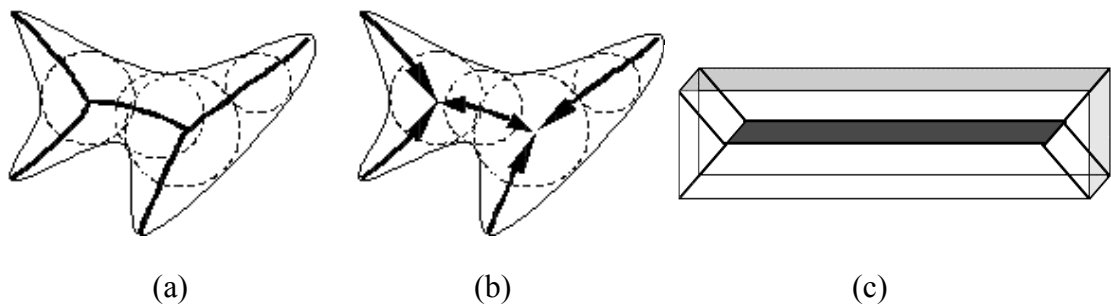

(a)   (b)   (c)

Figure 1 The Medial axis (a) and the shock graph (b) of a curve; the medial representation of a solid (c) may contain also surface elements

In applications that require curvilinear structures, such as animation [50] and virtual medicine [51], the medial representation should be as thin as possible, such that it may coded in a linear skeleton. Many methods have been proposed for extracting a curvilinear skeleton [16][26][49][51], also known as *curve skeleton* or *centerline* [43]. Depending on the complexity of the curve skeleton extraction, many approaches focus on *2D* images and employ thinning techniques [38], such as boundary erosion [24] distance transform [8], which correspond to a rough approximation of the medial axis. The thinning approach to *3D* objects is mainly based on a constrained distance transform [50] or a potential field of an object as discussed in [16]. Main drawback of these structure is that the resulting curve skeletons might not preserve the object

topology and, even, lose the connectedness of the descriptor. Thus, the resulting skeletal graph representation, which, for example, may be obtained through the approach proposed in [46], could have an arbitrary number of cycles, independently of the object handles. Moreover, the need of having a curve-like description of the shape conflicts with the goal of having an exact reconstruction of the object. The curvilinear structures proposed in figure 2, which are obtained using the potential field erosion proposed in [44], show some examples of this phenomenon.
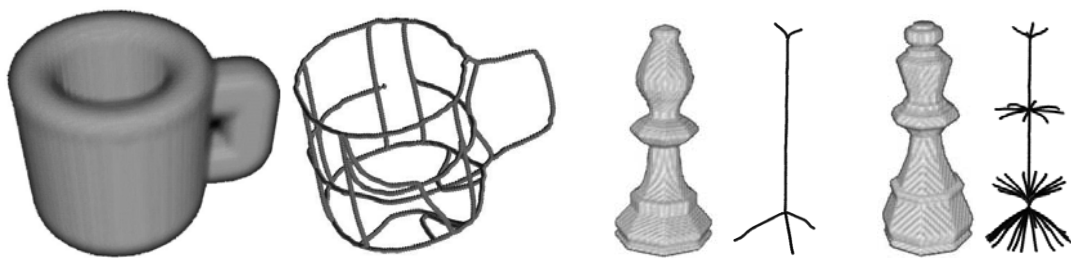

Figure 2 Three objects and the corresponding curve skeletons, (these images are available at http://www.caip.rutgers.edu/vizlab.html)

Differential topology suggests another approach to shape description, which mainly relates to Morse theory [19][31]. Since a finite collection of level sets of a smooth function f defined on the surface is sufficient to fully describe the surface shape, the level set evolution of f may be coded in a topological graph, called a Reeb graph, that collapses in a point each component of the level sets [35]. More formally, the Reeb quotient space of a surface S with respect to a real valued function f has been defined as

the quotient space that identifies two points P, Q of S if they have same value of f and belong to the same connected component of the pre-image of f, (f^{-1}). Then, the Reeb quotient space may represented as a graph, in which nodes represent the critical levels of f that correspond to the creation, merging, split or deletion of a contour, and arcs are associated to surface portions that connect two critical levels. Moreover, an orientation may be associated to each arc, according to the increasing direction of the function f. In figure 3, an example of the Reeb graph representation of a mechanical model is shown with respect to the height function f, in particular, figure 3(b) represents the contour levels of f, while figure 3(c) highlights the Reeb quotient space obtained collapsing each contour in its centre of mass; finally the Reeb graph is shown in figure 3(d).

The Reeb graph may be represented by a 1D structure that is topologically equivalent to the original shape and roughly describes the shape features that are relevant with respect to the function chosen. Since also geometric information may be stored in the graph. it is more satisfactory than the simple knowledge of the global object topology [28]. Furthermore, the flexibility of the choice of the mapping function makes this graph suitable for different tasks, such as shape analysis [1][42][25], similarity [21] and matching [6] and different application contexts, such as CAD [3], free-form meshes [1][25], contours [42], medical imaging [41] and DTM[10], where the Reeb graph is also known as *contour tree*. Finally, an overview of the possible choices of the mapping function (e. g. height distance, geodesic distance, distance from a point in the space, geodesic distance from curvature extrema, etc.) and a discussion on their properties and efficacy has been proposed in [5].
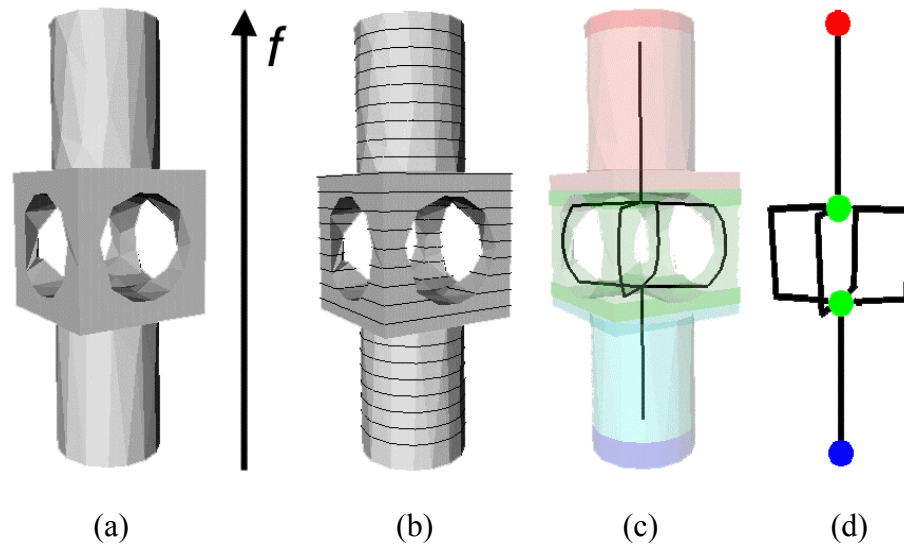
Figure 3 In (b) the contouring of the object (a) with respect to the direction f is shown; the quotient space obtained by collapsing the level sets and the Reeb graph representation are depicted in (c) and (d), respectively

2.2 Shape matching

Concerning 3D shapes, there is a great number of techniques for shape matching. The methods developed so far vary from coarse filters suited to browse very large 3D repositories on the web, to domain-specific approaches to assessing similarity of part models containing semantic as well as structural information.

A method for a coarse estimation of the similarity between two 3D models has been proposed in [11]. The authors propose to describe the shape of a 3D model with respect to its convex hull and bounding box. Four simple descriptors are used: the ratio of the longest to the shortest axis of the bounding box; the ratio between the area of the

model and the area of the convex hull; the percentage of the convex hull volume not occupied by the original model, and, finally, the hull compactness; that is the ratio of the hull's surface area cubed over the volume of the convex hull squared. Since this approach is robust to small model shape perturbations and is computationally efficient, it is a good coarse filter in the application context of the CAD/manufactured 3D model retrieval; on the contrary the coarse nature of this shape descriptor does not allow an accurate structural analysis of the object features.

The method proposed in [46] compares two skeletal structures, which are obtained through an erosion process from a 3D model voxel representation, by following the approach described in [43]. The basic idea of such an approach is to transform the graph extracted from the skeleton in a rooted tree and, then, to map the nodes of two trees visiting them from their roots. The mapping process is based on an indexing mechanism that maps the topological structure of a tree into a low-dimensional vector space based on an eigenvalue characterization of the connectivity of the tree.

In [3] the comparison between CAD models, based on the Multiresolutional Reeb Graphs (MRG) similarity computation proposed in [21] is presented. The similarity estimation between 3D models is processed using a coarse-to-fine strategy preserving the consistency of the graph structures, which results in establishing the correspondence between the parts of objects. The basic idea is to demonstrate the efficacy of the MRG to the problem of the manufacture-model retrieval. Some experiments has been proposed to show the performance of the MRG technique on primitive CAD models, such as cubes and spheres, on more complex models, such as

LEGO and mechanical parts, and finally, on complex CAD models. The results of such experiments show that MRG comparison produce rather acceptable results, nonetheless several problems arise from this technique. For example, the 3D model has to be two-manifold; furthermore, the comparison process may produce false positive results and it is more sensitive to the geometry of a model rather than its topology. The constraint of using only two-manifold models could be relaxed, but problems dealing with the computational complexity and the shape representativeness of the graph may occur.

The same authors in [4] presented a new methodology to compare two manufactured models; however, their method could be applied to free form 3D models too. Here, a hierarchical decomposition of the object features is stored in a rooted tree where each node represents a feature and its descendents corresponds to its sub-features. Since the nodes of the tree represent parts of the object and the edges connecting two nodes represent either the adjacent relation or the containment relation between them, the feature/sub-feature rooted tree is a representation of the structure of the object. Therefore, under the assumption that the similarity between two features is closely related to the similarity between their sub-features, the similarity between two 3D objects is evaluated through the comparison of the corresponding rooted-trees and its efficacy has been shown.

Finally, also the shape matching method we have proposed in [6] is based on the Reeb graph structure. On the contrary to the approaches previously described, such a method directly works on the graph structure and deals with the graph comparison problem using the notion of error tolerant sub-graph isomorphism proposed in [9].

Since the exact computation of the maximal common sub-graph is a *NP-complete* problem, some heuristics that simplify the matching algorithm and locally solve the problem, have been introduced. In particular, these heuristics may modularly be inserted in a more global process of extraction of the maximal common sub-graph, as we will show in section 3.2. Due to intuitiveness of the Reeb graph for free-form models, such as animals and human bodies, until now this method have been used for comparing such a class of objects, while in this work we tackle the problem of adopting that method for mechanical models.

3   Our approach to 3D object retrieval

First of all we discuss how to describe the shape of 3D objects represented by a closed triangle mesh and use the resulting coding for similarity evaluation and matching purposes.

As shown in section 2, skeletons and Reeb graphs provide an efficient coding of the surface shape, which may be represented as a directed graph. This property may be exploited during the graph comparison process, in fact it is reasonable that two arcs can be mapped only if they have same orientation. Moreover, since each node also identifies the sub-graph starting from it as shown in [6], its relevance in the graph depends on the size of the sub-graph. Therefore, the graph matching is accomplished through a priority queue that takes into account the relevance of the graph entities, where the relevance of an arc is given by the difference of the function values calculated along its end nodes. The comparison of two shapes may be effectively performed on the graph representation instead of the whole geometric model adding to each arc (and node) a set

of attributes, which represent the geometry and topology associated to them. Finally nodes and arcs mapping obtained through the error tolerant sub-graph isomorphism allows sub-part object mapping.

3.1 From a shape to a graph representation

To be effectively available for shape matching purposes a structure should be independent of object position, rotation and scaling. For example, skeletons satisfy these requirements, while for the Reeb graph the choice of the mapping function has to be restricted to those functions that do not depend on the shape embedding in the space. As proposed in [46] and [6] both a skeleton and a Reeb graph may be represented as an a-cyclic, directed graph. However, the skeletal structure requires a number of simplification steps and artefacts [46], which might alter the topology of the signature, while the Reeb graph is mathematically well-defined and there is a strict relationship between the object topology and the graph structure; therefore we have chosen the second structure for our experiments.

Beside the topological information stored in the graph structure, attributes have been associated to arcs and nodes to represent the main geometric characteristics of the corresponding features. Therefore the Reeb graph better describes the shape, the better the function does. In Figure 4, the Reeb graph of two models with respect to the distance from the centre of mass (barycentre) of the object, the geodesic distance from the curvature extrema in [14] and the integral geodesic function introduced in [21] is proposed. The two models are almost identical, except on the handle. In this case, the Reeb graph based on a spatial-based function such as the distance from the centre of

mass is less sensitive to a small change of the object topology (the breaking of the handle) than those provided by surface-based distances as the geodesic one.
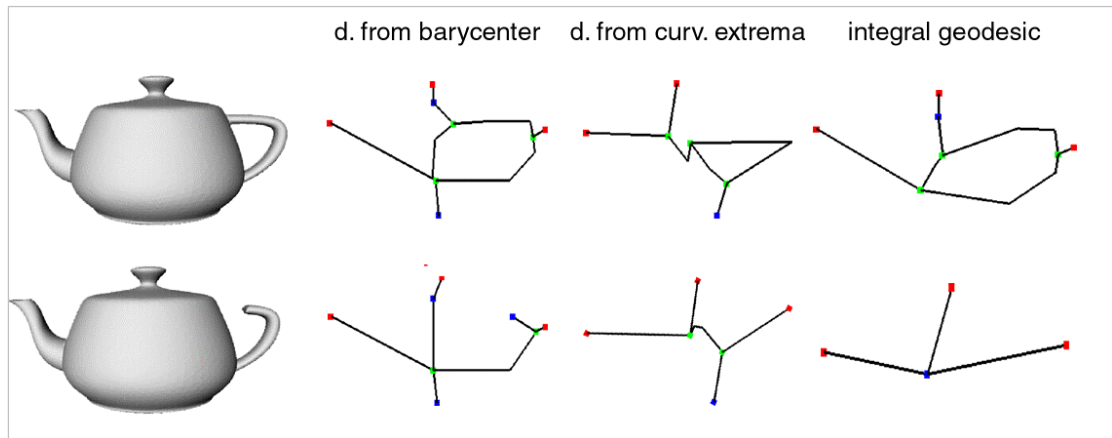

Figure 4 The Reeb graph of two models with respect to different functions

On the contrary, functions based on the surface shape, such as the geodesic distance, highlight object protrusions and cavities and are useful in those contexts where an object has to be recognised despite curling or stretching deformations.

The computation of the Reeb graph is performed through the contouring approach proposed in [2]. As shown in [21], a multi-resolution representation of the Reeb graph is given by computing a sequence of Reeb graphs at different resolutions, which are obtained by doubling, at each step, the number of slicing contours. In our approach, critical areas are considered instead of critical points. A node is associated to each critical area, while arcs are detected through a region growing process.

3.2 Graph matching

By the assumption that our graph representation encodes the main shape features and the most significant spatial relations between them, the target of our approach is to map together the structural parts of our signature; that is achieved through an isomorphism between two graphs. Such a graph isomorphism should highlights how much the two shape overlap. As discussed in [30][6], the existence of a graph isomorphism implies that the graphs must be equivalent; however, such a strong requirement can be relaxed using a weaker similarity measure based on the weak notion of isomorphism proposed in [30], where the definition of the Error Tolerant Graph Isomorphism (ETGI) is introduced to estimate the similarity between two 3D models. By an intuitive point of view, constructing an ETGI means obtaining a common sub-graph as big as possible, that is a Maximum Common Sub-graph (MCS). Unfortunately, the construction of the MCS is a well-known *NP-complete* problem; thus, its exact computation is time consuming, when the shape descriptors are composed by a large numbers of nodes and edges. Therefore, several strategies and heuristic assumptions have been adopted to simplify this problem [30][43][6].

In this section we discuss how the heuristics we have introduced into the graph matching algorithm in [6], may be viewed as an approximation of an algorithm for graph comparison that exactly computes the MCS.

The simplest algorithm for the MCS construction between two graphs A and B is the enumeration of all the possible mappings among the nodes of A and B; unfortunately this simple method does not evidence how heuristics based on object

topology and geometry information may approximated the MCS. Thus, in the following, we propose a general graph matching approach, which extends the method described in [6] and characterises the MCS problem in a modular framework, allowing heuristics based on the shape structure. Moreover, we recall that the edge orientation induces a sub-graph for each node and, once two nodes are mapped, also their sub-graphs must verify the isomorphism constraints. We observe that the extraction of the MCS satisfies the following considerations:

1. the maximum common sub-graph $MCS_{a \to b}$ originated mapping two nodes $a \in A, b \in B$ is obtained by recursively considering, among all possible pairs of children of a and b, the one that originates the best induced common sub-graph. We name that pair (a'_i, b'_j), $a' \in A$, $b' \in B$. The element (a'_i, b'_j) may be added to the isomorphism map; moreover, in order to continue the $MCS_{a \to b}$ construction, also all pairs obtained from the children of a'_i and b'_j have to be joined to the pairs of the children of a and b.

2. For each single pair (a, b), there exists another pair of nodes (a', b'), with $a \neq a'$ and $b \neq b'$, such that $MCS_{a \to b, a' \to b'}$ is bigger or equal than $MCS_{a \to b}$. Then, the maximum common sub-graph $MCS_{a \to b, a' \to b'}$ is obtained by recursively expanding, at the same time, both $a \to b$ and $a' \to b'$ as explained in the previous point.

3. More generally, denoting M be the set of all possible bijective mappings among the nodes of A and B and MCS_m the maximum common sub-graph induced by a map $m \in M$, there exists $m' \in M$ such that $MCS_{m'}$ is equal or bigger than MCS_m. In particular, since the set M is finite, the maximum common sub-graph of A and B is always induced by at least a map.

Starting from these considerations and recalling that the input of the matching algorithm is an attributed, a-cyclic and directed graph, heuristics may be introduced either in all the three steps of the previous pipeline or once at time, furthermore, the pipeline assures that improving the heuristics results in a better approximation of the MCS. The heuristics we have proposed in [6] introduce a simplification of the matching algorithm by considering a local solution of the problem and strongly reducing the computational complexity from exponential to cubic ($O(n^3)$, where n is the number of graph nodes). For example, the problem of extracting the maximum common sub-graph of a node pair is reduced by considering a node description that measures the importance of such a node by taking into account both the attribute values and the number of nodes/edges of the induced sub-graph. In addition, through considerations on the distribution of the graph nodes with respect to its attributes, an initial map among the nodes of the two graphs is detected and the common sub-graph is achieved by starting from that map.

In Figure 5 an example of our matching method is proposed: in Figure 5(a) the initial state and the first best candidate pair, which is represented by a filled square, are shown, while the final matching is depicted in Figure 5(b).
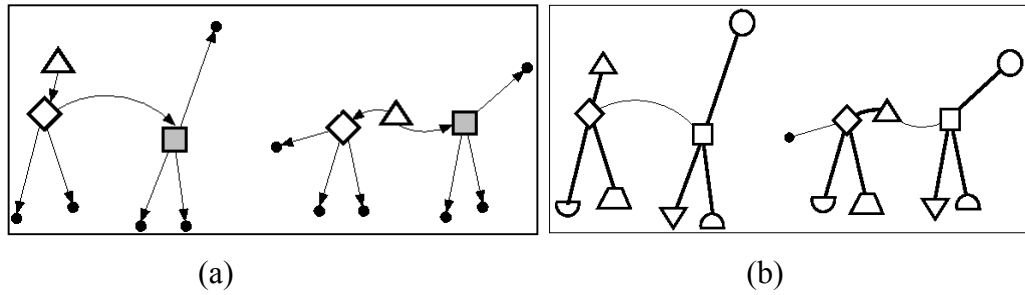
(a)   (b)

Figure 5 The matching algorithm

Finally, we observe that the usual definition of the MCS in [9] does not consider the graph attributes, thus the MCS maximizes the number of nodes and edges involved in the match but does not takes into account their relevance in the shape. This implies that the choice of the representative of the MCS is important and, in our approach, the MCS is chosen as that minimizes the sum of the differences of the edge pairs. In Figure 6 two possible choices of the mapping that individuates the maximum common sub-graph are proposed; both sub-graph configurations are topologically identical but the mappings are different; in our assumption the best mapping is that in Figure 6(b) because it minimizes the sum of the difference of the edge pairs.
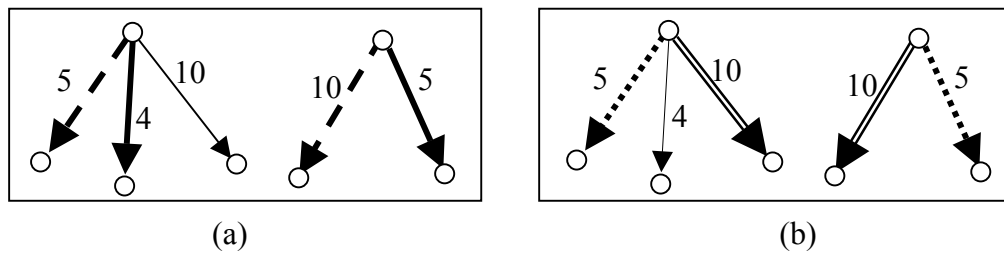

(a)   (b)

Figure 6 Two possible maximum mappings between two simple trees are shown;

numbers represent the value of the edge attributes while the line style represents the

edge mapping

3.3 Distance measure

The definition of a distance between two graphs is a well-known problem in graph theory; in particular, the approach proposed in [9] considers the maximum common sub-graph as the term of comparison between two graphs. According to that, in [6] we proposed a distance that evaluates how far two graphs are; in particular, the bigger the common sub-graph defined by the error tolerant isomorphism is, the smaller the distance should be. More formally, the distance measure is a real function $d:GxG\rightarrow[0,1]$ where G represents the set of all the attributed graphs. Therefore, given two graphs G_1 and G_2 and their common sub-graph S, the distance d is defined as follows:

$$d(G_1,G_2) = 1 - \frac{\sum_{e \in S} 1 - \frac{\left| \mu_1^{-1}(e) - \mu_2^{-1}(e) \right|}{\alpha}}{\max(|G_1|, |G_2|)}$$

where μ_i^{-1} are the attribute values of an edge in the i-th graph and the symbol $| \bullet |$ indicates the number of edges of a graph.

Such a distance takes into account both the structure and the edge distribution of the two graphs. However, from a mathematical point of view, this distance is a semi-metric: in fact, it satisfies the properties of uniqueness, identity, non-negativeness, and symmetry but does not verify the triangular inequality.

4   Results and discussion

As discussed in section *3.1*, the behaviour of the different choices of the function in the Reeb graph representations has to be taken into account during the similarity analysis: in fact each function emphasizes different aspects of the object shape.

Figure 7 highlights how the choice of the function in the Reeb graph representation influences the matching results. In fact, the topology of the teapot has been modified and the graphs result much different. The graph obtained through the distance from the barycentre function is a representation of the spatial distribution of the object with respect to its centre of mass: even if a part of the handle has been removed, the remaining part folds on itself, generating a critical points in the Reeb function. On the contrary, the graph based on the integral geodesic does not take into account the spatial embedding, thus the broken handle of the teapot results in a maximum critical point with respect to the geodesic distance, neglecting the shape of the handle itself.

d. from barycentre   d. from curv. extrema   Integral geodesic

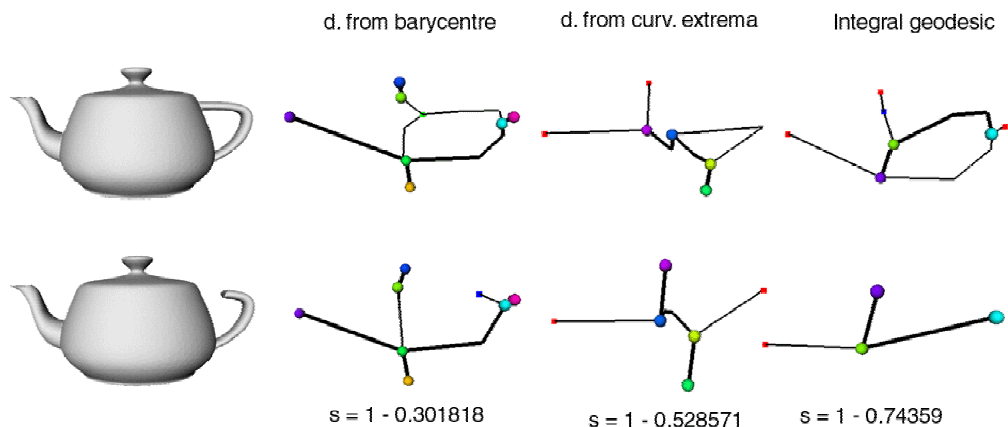s = 1 - 0.301818   s = 1 - 0.528571   s = 1 - 0.74359

Figure 7 Matching between the three Reeb representations of the teapot and its modified version proposed in Figure 4 and their similarity evaluation. Thick arcs and nodes with same colour represent the graph mapping

Concerning the distance from the curvature extrema, the modification of the teapot handle results in a new curvature extreme generating a new maximum critical point. Since in a manufacturing model high curvature points may be not isolated and individuate large regions, above all in correspondence of sharp features, the latter function does not seem to be a good choice for the mapping function in the CAD context.

Experimental results of our matching method obtained by using the CAD models in the two databases (http://www.designrepository.org/SM03 and http://www.designrepository.org/DECT03) proposed in [3] and [4] are shown in Figure 8, where the five top objects retrieved by our matching algorithm on two query models (a linkage and a socket) are shown. In our experiments the algorithm performs more than 10.000 graph comparisons in less than 10 seconds on a AMD Athlon 1GHz with 512 Mb of RAM. Results are arranged according to their similarity value with respect to the query models, in decreasing order from left to right. For both, we compare the Reeb graph representations with respect to the choice of the mapping function f: line a) corresponds to the distance from the barycentre while line b) to the integral geodesic distance.
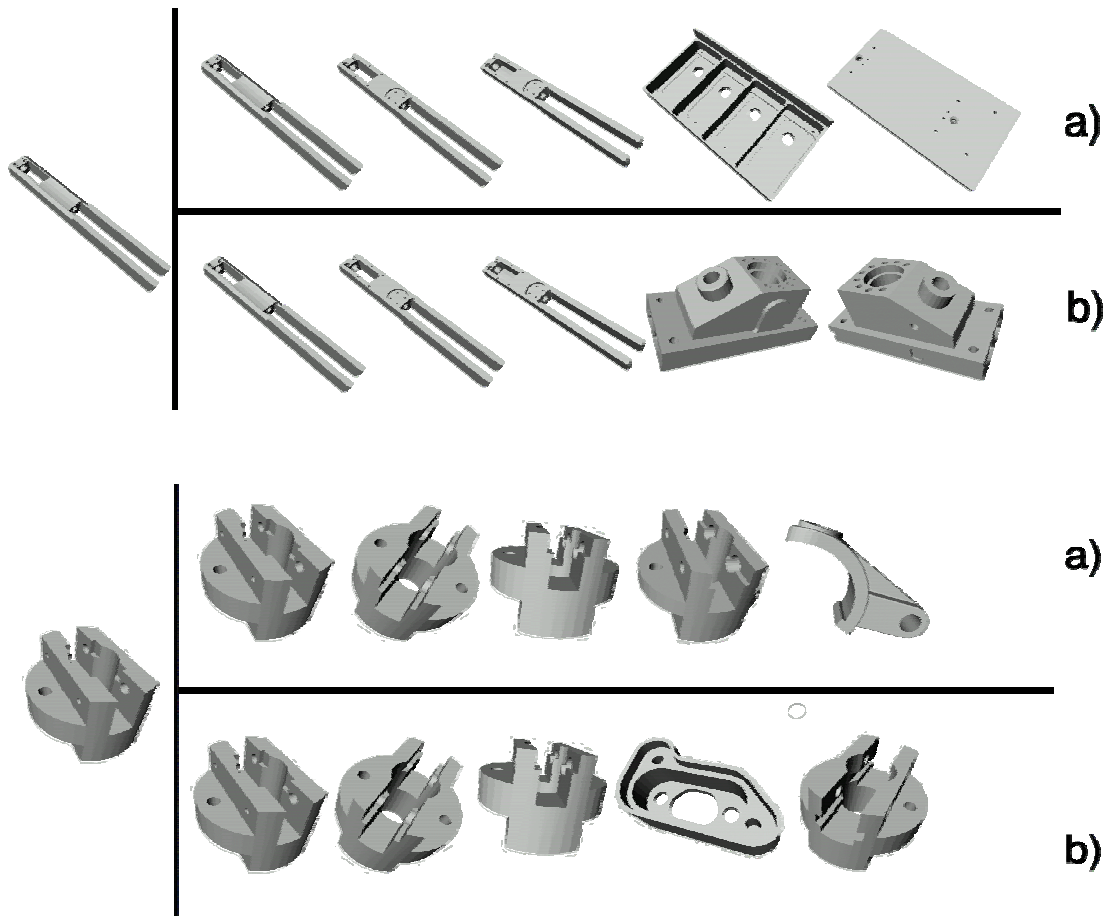
Figure 8 Matching results for two query models

Some comments can be done. Since the matching approach is based on both the Reeb graph representation and the edge attributes, for each function, the best match was the model itself. Moreover, each family of objects is correctly detected, even if some false positives are possible; see Figure 9 for the representation of the object groups in the database. For instance, the query results of the linkage correctly recognize in the first three top positions all similar linkages; while the choice of other two models depends on the function. In particular, the distance from the barycentre favours the choice of models whose shape is lengthened while the integral geodesic distance selects

objects having similar features, even if spatially distributed in a different manner. This fact is further emphasized for the socket model, where the fourth object retrieved, which has the same number of holes and the same smoothed appearance of the query model, is preferred to a socket with a different number of holes.
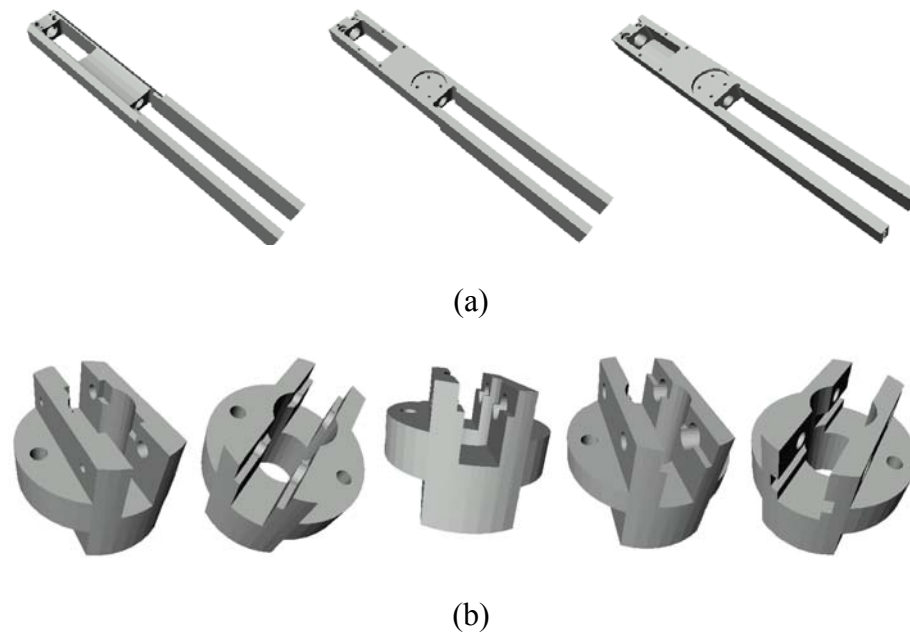

(a)

(b)

Figure 9 The groups, in our database, of the linkage models (a) and the socket ones (b)

In figure 10, we show the Reeb graph of two objects both with respect to the distance from the barycentre, pictures (b,e), and with respect to the integral geodesic distance, (c,f). Since the subparts of the graphs (c) and (f), which are highlighted in the circles, are almost identical, we observe that the graph (f) does not distinguishes the sharp corner highlighted in (d) from the corresponding smooth region in (a). On the contrary, since the distance from the barycentre classify the sharp corner as a minimum,

a new arc appear in (e) and, indeed, the graph representations in (b) and (e) differ more significantly.
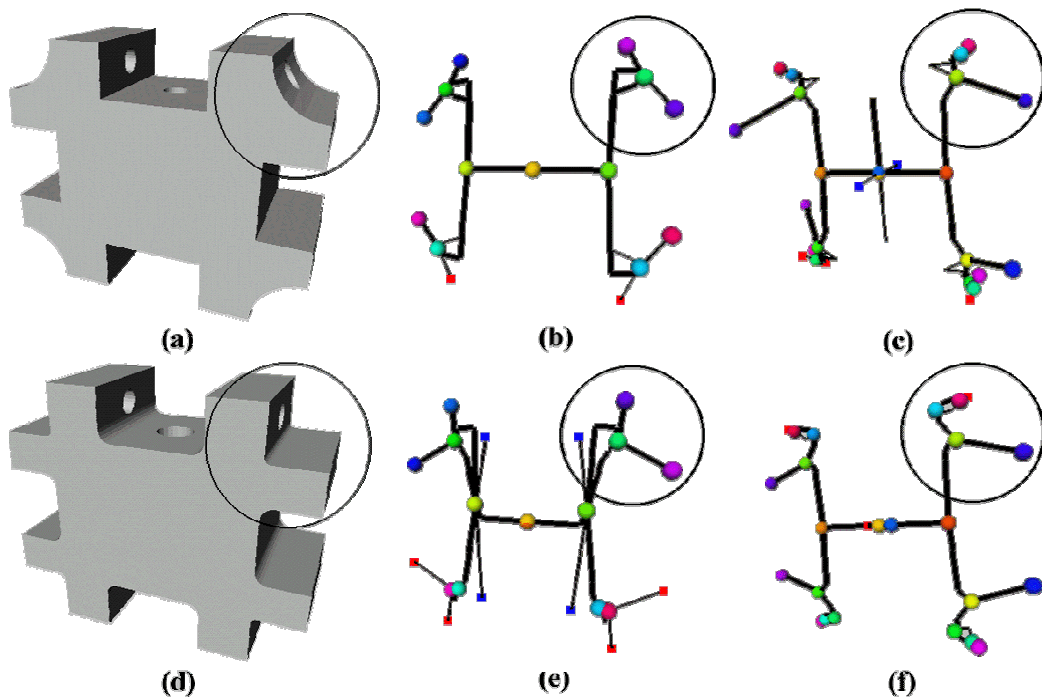

Figure 10 Matching of the Reeb graphs of the objects (a) and (d) with respect to the distance from the barycentre (b) and (e) and the integral geodesic distance (c) and (f)

The use of topological structures to represent model features allows a good representation both for topology and structural aspects, while the ability of taking into account both topological and geometrical/structural aspects of the model shape strongly depends by the comparison process adopted. Finally, we observe that mechanical models may differ from small features, number of holes or smoothness: however, also

in these cases our algorithm has performed in a satisfactory manner, emphasizing these differences and grouping objects with similar shape.

A statistical description of the performance of our method is proposed in Figure 11 and Figure 12, where the queries to our database are represented with respect to a standard evaluation of information retrieval systems: the precision/recall curve. In particular, the *recall* is given by the proportion of the relevant models retrieved in answer to a query while the *precision* represents the proportion of retrieved models that are actually relevant, [47]. In other words, the recall and precision descriptors attempt to measure the *effectiveness* of the retrieval method measuring the ability of the system to retrieve relevant documents and discard non-relevant ones.

In Figure 11 we show the matching results obtained with our graph comparison method with respect to different resolutions of the Reeb graph. In particular, the Reeb graph has been extracted in a multi-resolution way, computing, respectively, 16, 32 and 64 subdivisions of the interval $[f_{min}, f_{max}]$. The results in Figure 11(a) are obtained using the distance from the barycentre (DB), while Figure 11(b) shows the results with respect to the integral geodesic distance (IG). We observe that the Reeb graph with respect to distance from the barycentre performs better at a lower resolution while the one with respect to the integral geodesic distance improves when the number of subdivisions of $[f_{min}, f_{max}]$ increases. This fact is not surprisingly because the distance from the barycentre induces a uniform slicing of the object that highlights the more the main shape structure of the object, the rougher the slicing is. On the contrary, since contour levels of the integral geodesic distance concentrate on the object protrusions

and cavities, it induces a non-uniform surface slicing and the resulting Reeb graph codes more handles and shape features the more the number of contour levels increases. This fact, emphasises, once more, the different nature of the mapping functions: spatial based the first and shape based the second.
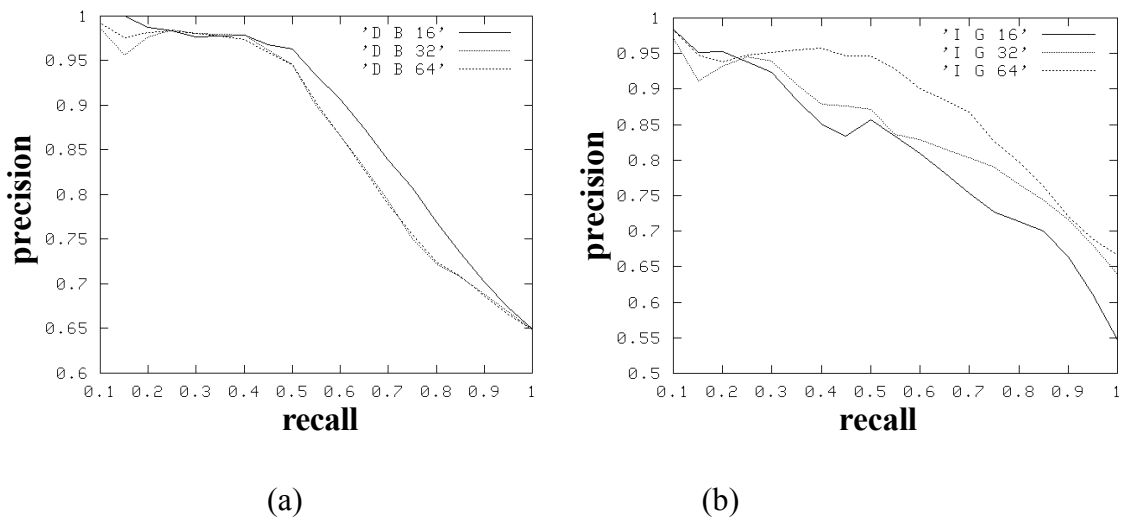

Figure 11 Multi-resolution matching approach with respect to the distance from the barycentre (a) and the integral geodesic distance (b)

In Figure 12 the results of our approach are compared with those obtained with the spherical harmonics method in [16]. Results of the method in [16] were obtained using the executables available at [53] and adopting the same shape classification and the same database when testing our method. When compared with our method, the approach based on spherical harmonics globally performs very well and, in general, the object classes are correctly recognised. Nevertheless, we have observed that the distinction provided by the Reeb graph structure is finer than that of the spherical harmonics and individuate the object parts that better overlap. For instance, the models

in figure 13 do not belong to the same class of our database but, being both elongated, they are not distinguished by the spherical harmonic descriptor while the Reeb graph correctly classify them.
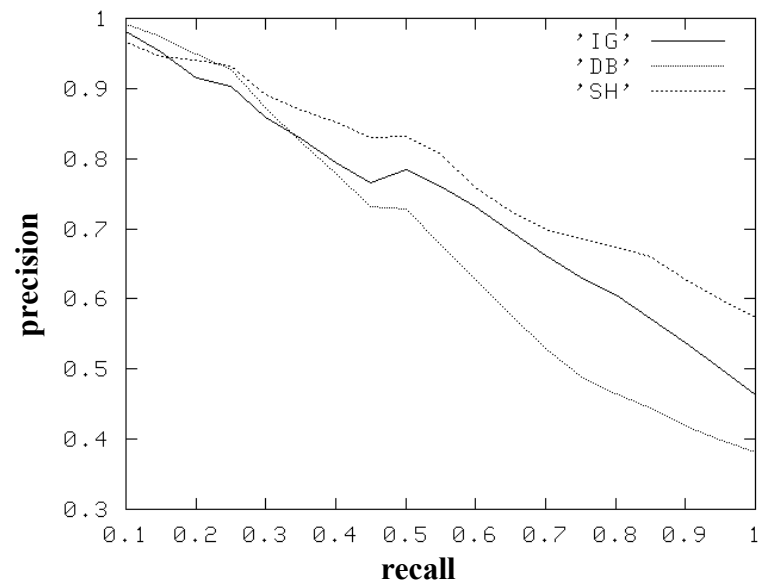

Figure 12 The precision/recall curve of the graph matching with respect to the distance from the barycentre, the integral geodesic distance and the spherical harmonics method for our database, over 200 models of CAD and free form objects
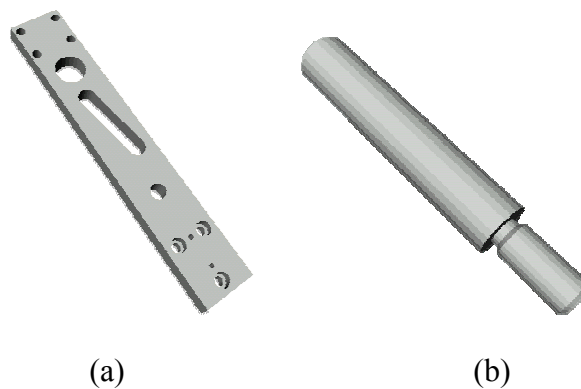

(a)   (b)

Figure 13 Two CAD models

Finally, we highlight that, differently from the approach proposed in [21] and adopted in [3], our method uses the graph representation induced by the Reeb graph instead of a similarity measure deduced on the surface segmentation. This fact allows the construction of a not necessarily connected common sub-graph, which is able to detect and map together similar parts of the model object (partial matching), and makes the algorithm robust with respect to slight structural and topological deformation. Therefore, the proposed approach should not be considered as a coarse filter but as a finer shape analysis tool where structure and topology are taken into account.

Moreover, even if the adopted matching approach is mainly based on the topological information stored in the graph, as a future development we are planning to consider a greater number of geometric attributes, which should improve the results so far obtained.

5   Conclusions and future work

No existing shape descriptor satisfies to all the 'ideal' requirements for shape matching. In fact, we have shown that curve skeletons may be topologically non equivalent to the original shape and, both curve skeletons and Reeb graphs, may depend on shape details. On the contrary spherical harmonics are more stable but do not allows the reconstruction of the original model and there is not correspondence between the descriptor and the shape of the object subparts. Furthermore, we have shown that matching methods based on skeletal-based descriptors are better suitable for tasks for

which it is fundamental to decompose the shape in salient portions, while other approaches, such as those based on shape distributions and spherical harmonics [16][39], better performs in retrieval tasks if partial matching and reasoning about subparts differences is not needed.

Open issues of our graph matching framework are how to improve the graph comparison method; for example we are planning to consider a larger number of attributes and define a distance measure that is also a metric. Moreover, our approach is available only for closed and manifold triangle meshes. This fact implies that it is not suitable for triangle soups such as it is easy to find in the Internet repositories. Currently we are investigating how to solve this problem and extend our method to generic surfaces with boundary.

Since the choice of the mapping function in the Reeb graph representation determines the characteristics of the resulting shape descriptor and, usually, each function highlights a shape property at time, we are investigating how to contemporarily use and integrate different mapping functions. Moreover, in our opinion it is necessary and useful to combine our method with other matching approaches, such as coarse filters [11], shape distributions [33] or spherical harmonics [16][39], in a multi-step approach which considers these filters to progressively refine the set of geometrically similar candidates, and/or a multi-modal query mechanism that could provide a combination of various measures of shape similarities, corresponding to function, form and structure analysis of 3D shapes. Finally, it would be interesting to test our method in other application fields, such as virtual human analysis and to deduce editing

operations from the graph isomorphism, in order to topologically and structurally align two different shapes.

Acknowledgements

References

[1] Attali, D. and Montanvert, A. (1997) 'Computing and simplifying 2D and 3D continuous skeletons', *Computer Vision and Image Understanding: CVIU*, Vol. 67, No. 3, pp. 261-273

[2] Attene, M., Biasotti, S., and Spagnuolo, M. (2003) 'Shape understanding by contour-driven retiling' *The Visual Computer*, Vol. 19, No. 2-3, pp. 127-138, Springer-Verlag

[3] Bespalov, D., Regli, W. C. and Shokoufandeh, A. (2003) 'Reeb graph Based Shape Retrieval for CAD', *Proceedings of the 2003 ASME Design Engineering Technical Conferences*

[4]   Bespalov, D., Shokoufandeh, A., Regli, W. C. and Sun, W (2003) 'Scale-Space representation of 3D models and topological matching', *Proceedings of 8th ACM Symposium on Solid Modeling and Applicaitons*, ACM Press, pp. 208-215

[5]   Biasotti, S., Marini, S., Mortara, M. and Patané, G. (2003) 'An overview on properties and efficacy of topological skeleton in Shape Modelling, *Proceedings of International Conference of Shape Modeling and Applications 2003*, IEEE Press, pp. 245—254

[6]   Biasotti, S., Marini, S., Mortara, M., Patané, G., Spagnuolo, M. and B. Falcidieno (2003) '3D Shape Matching through Topological Structures', *Proceedings of 11th Discrete Geometry for Computer Imagery conference, Lectures Notes in Computer Science 2886* (Sanniti di Baja, G., Svenssons S. and Nystrom I. eds), Springer Verlag, pp. 194-203

[7]   Blum, H. (1967) 'A transformation for extracting new descriptors of shape'. *Proceedings of Symp. Models for the Perception of Speech and Visual Form (W. W. Dunn, eds.)*, MIT Press, Cambridge, MA, pp. 362-380

[8]   Borgefors, G. (1996) On Digital Distance Transforms in Three Dimensions, *Computer Vision and Image Understanding*, Vol. 64, No. 3, pp. 368-376

[9]   Bunke, H. and Shearer, K. (1998) 'A graph distance metric based on the maximal common subgraph', Pattern Recognition Letters, Vol. 19, pp. 255-259

[10] Carr, H., Snoeyink, J. and Axen, U. (2000) 'Computing Contour Trees in All Dimensions', *Proceedings 11th Annual ACM-SIAM Symposium on Discrete Algorithm (SODA 2000)*, San Francisco, pp. 918-926

[11] Corney, J., Rea, H., Clark, D., Pritchard, J., Breaks, M. and MacLeod R. (2002) 'Coarse filters for shape matching', *IEEE Computer Graphics and Applications*, Vol. 22, No. 3, pp. 65-74

[12] Dey, T. K., Edelsbrunner, H. and Guha, S. (1999) 'Computational Topology. Advances in Discrete and Computational Geometry', (Chazelle B, Goodman J E, Pollack R, eds), *Contemporary Mathematics 223*, AMS, Providence, pp. 109-143

[13] Edelsbrunner, H., Harer, J. and Zomorodian, A. (2001) 'Hierarchical Morse Complexes for Piecewise Linear 2-Manifolds', *Proceedings ACM Symposium on Computational Geometry*, Medford, MA, pp. 70-79

[14] Falcidieno, B., Mortara, M., Patané, G., Rossignac, J. and Spagnuolo, M. (forthcoming) 'Blowing Bubbles for the Multi-Scale Analysis and Decomposition of Triangle-Meshes, *Algorithmica, Special issue on Shape Algorithmics*

[15] Falcidieno, B. and Spagnuolo, M. (1998) 'Shape Abstraction Paradigm for Modeling Geometry and Semantics'. *Proceedings of Computer Graphics International*, Hannover, pp. 646-656

[16] Funkhouser, T. , Min, P., Kazhdan, M., Chen, J., Halderman, A., Dobkin, D. and Jacobs, D. (2003) 'A Search Engine for 3D Models', *ACM Transactions on Graphics*, Vol. 5, N. 10, pp.??

[17] Gagvani, N. and Silver, D. (1999) 'Parameter controlled Volume Thinning', *Graphical Models and Image Processing*, Vol. 61, No. 3, pp. 149-164

[18] Giblin, P. J. and Kimia, B. B. (2003) 'On the local form and transitions of symmetry sets, medial axes, and shocks', *International Journal of Computer Vision*, Vol. 54, No. 1-3, pp. 143-157

[19] Guillemin, V. and Pollack, A. (1974) *Differential Topology*, Englewood Cliffs, NJ: Prentice-Hall

[20] Hamza, B. and Krim, H. (2003) 'Geodesic object representation and recognition', *Proceedings of 11th Discrete Geometry for Computer Imagery conference*, *Lectures Notes in Computer Science 2886* (Sanniti di Baja, G., Svenssons S. and Nystrom I. eds), Springer Verlag, pp. 378-387

[21] Hilaga, M., Shinagawa, Y., Kohmura, T, and Kunii, T. L. (2001) Topology Matching for Fully Automatic Similarity Estimation of 3D Shapes. *Computer Graphics (SIGGRAPH '01 Proceedings)*, Los Angeles, pp. 203-212

[22] Hoffmann, C (1989) *Geometric and Solid Modeling*, Morgan Kaufmann

[23] Kimia, B., Tannenbaum, A. and Zucker, S. (1995) 'Shapes, shocks, and deformations, I', Computer Vision, Vol. 15, pp. 189-224

[24] Lam, L., Lee, S.-W. and Suen, C. Y. (1992) 'Thinning methodologies − a comprehensive survey', *IEEE Trans. On Pattern Analysis and Machine Intelligence*, Vol. 14, No. 9, pp. 869-885

[25] Lazarus, F. and Verroust, A. (1999) Level Set Diagrams of Polyhedral Objects. *Proceedings of Solid Modeling*, pp.130-140

[26] Liu, A., Bullitt, E. and Pizer, S. (1998) '3D/2D Registration via Skeletal Projective Invariance in Tubular Objects', *Proceedings of Medical Image Computing and*

Computer-Assisted Intervention, Lectures Notes in Computer Science 1496 (Wells, W. M., Colchester, A. and Delp, S. eds), Springer Verlag, pp. 194-203

[27] Lounsbery, M., DeRose, T. D. and Warren, J. (1997) 'Multiresolution analysis for surfaces of arbitrary topological type', *ACM Trans. on Graphics*, Vol. 16, No. 1, pp. 34-73

[28] Mäntylä, M. (1988) *An Introduction to Solid Modeling*, Computer Science Press

[29] Massey, W. (1967) '*Algebraic Topology: An Introduction*' Harcourt, Brace & World, Inc.

[30] Messmer, B. T. and Bunke, H. (1998) 'A New Algorithm for Error Tolerant Subgraph Isomorphism Detection', *IEEE Trans. on Pattern Analysis and Machine Intelligence*, Vol. 20, No. 5, pp. 493-504

[31] Milnor, J. (1963) *Morse Theory* Princeton University Press, New Jersey

[32] Nackman, L. R. and Pizer, S. (1985) 'Three-dimensional shape description using the symmetric axis transform: I: Theory', *IEEE Transactions on Pattern Analysis and Machine Intelligence*, Vol. 7, pp. 187-201

[33] Osada, R., Funkhouser, T. , Chazelle, B. and Dobkin, D. (2001) 'Matching 3D models with shape distributions', *Proceedings of International Conference of Shape Modeling and Applications 2001*, pp. 154-166

[34] Piegl, L. A. and Tiller, W. (1997) *The Nurbs Book, Monographs in Visual Communications*, Springer Verlag

[35] Reeb, G. (1946) 'Sur les points singuliers d'une forme de Pfaff complètement intégrable ou d'une fonction numérique'. *Comptes Rendus Acad. Sciences*, Paris, Vol. 222, pp. 847-849

[36] Requicha, A. A. G. (1999) *Geometric Modeling: A first course*, University of Southern California

[37] Renner, G. and Stroud, I. A. (1997) 'Medial surface generation and refinement', Proceedings of the 5th IFIP TC5/WP5.2 Workshop on geometric modelling in CAD on product modelling for computer integrated design and manufacture, pp. 371-383, Airlie, Virginia, US

[38] Rosenfield, A. (1998) *Digital geometry: introduction and bibliography*, chapter 1, Klette, R., Rosenfield, A. and Sloboda, F. (eds), Springer-Verlag

[39] Saupe, D. and Vranič, D. (2001) '3D model retrieval with spherical harmonics and moments', DAGM 2001, pp. 392-397

[40] Serra, J. (1982) *Image analysis and Mathematical Morphology*, Academic Press

[41] Shattuck, D. and Leahy, R. (2001) 'Automated graph based analysis and correction of cortical volume topology', *IEEE Trans. on Medical Imaging*, Vol. 20, No. 11, pp. 1167-1177

[42] Shinagawa, Y., Kunii, T. L. and Kergosien, Y. L. (1991) 'Surface Coding Based on Morse Theory' *IEEE Computer Graphics & Applications*, Vol. 11, No. 5, pp. 66-78

[43] Shokoufandeh, A., Dickinson, S. J., Siddiqi, K. and Zucker, S. W. (1999) 'Indexing using a spectral encoding of topological structure', *Proceedings of the IEEE Conference on Computer Vision and Pattern Recognition*, pp. 491-497

[44] Singh, V., Silver, D. and Cornea, N (2003) 'Real-Time Volume Manipulation' *Proceedings of 3rd International Workshop on Volume* Graphics, Fujishiro, I, Mueller, K. and Kaufman, A. (eds), pp.

[45] Svennson, S. and Sanniti di Baja, G. (2002) 'Curve skeletonization of surface-like objects in 3D images guided by voxel classification, *Pattern recognition Letters*, Vol. 23, No. 12, pp. 1419-1426

[46] Sundar, H., Silver, D., Gagvani, N. and Dickinson, S. (2003) 'Skeleton Based Shape Matching and Retrieval', *Proceedings of International Conference of Shape Modeling and Applications 2003*, IEEE Press, Seoul, May 2003, pp. 130-139

[47] Van Rijsbergen, C. J. (1979) *Information Retrieval*, Butterworth, (online: http://www.dcs.gla.ac.uk/Keith/Preface.html)

[48] Veltkamp, R. C. and Tangelder, J. W. H. (2003) 'Polyhedral model retrieval using weighted point sets', *Proceedings of International Conference of Shape Modeling and Applications 2003*, IEEE Press, pp. 119-289

[49] Verroust, L. and Lazarus, F. (2000) 'Extracting skeletal curves from 3D scattered data', *The Visual Computer*, Vol. 16, No. 1, pp. 15-25

[50] Wade, L. (1997) *Automated generation of Control Skeletons for use in Animation*, PhD Thesis, The Ohio State University

[51] Zhou, Y. and Toga, W. (1999) 'Efficient skeletonization of 3D volumetric objects' *IEEE Trans. on Visualization and Computer Graphics*, Vol. 5, No. 3, pp. 197-209

[52] Zuckerberger, E., Tal, A. and Shlafman, S. (2002) 'Polyhedral surface decomposition with applications', *Computer & Graphics*, Vol. 26, pp. 733-743

[53] http://www.arion-dl.org/AIM@SHAPE/

[54] http://www.cs.princeton.edu/~mkazhdan/HarmonicSignatures/